Available online at www.sciencedirect.com
SCIENCE DIRECT®
Optics Communications 262 (2006) 224–228
OPTICS COMMUNICATIONS
www.elsevier.com/locate/optcom

Quantum trajectory studies of many-atom and finite transit-time effects in a cavity QED microlaser or micromaser

C. Fang-Yen *

George R. Harrison Spectroscopy Laboratory, Massachusetts Institute of Technology, 77 Massachusetts Avenue, Room NW14-1215, Cambridge, MA 02139, United States

Received 10 October 2005; received in revised form 1 December 2005; accepted 23 December 2005

Abstract

Studies of microlasers and micromasers generally assume that at most one atom is present in the resonator and transit times are much shorter than cavity lifetimes. We use quantum trajectory simulations to investigate the behavior of a microlaser/micromaser in which multiple atoms may be present and atom transit times can be comparable to the cavity decay time. Many-atom events are shown to destroy trap state resonances even for a mean intracavity atom number as small as 0.1. Away from trap states, results for mean photon number agree with a single-atom, weak-decay theory. However the variance of the photon number distribution increases relative to micromaser theory by an amount proportional to the product of the interaction time and cavity decay rate. This excess variance is interpreted as resulting from cavity decay during the atomic transit time.

1. Introduction

The cavity QED microlaser [1,2] is a laser in which the atom-cavity coupling is coherent (well-defined). It is the optical analogue of the micromaser [3], a device which has drawn great interest due to its unusual features such as sub-Poisson statistics [4] trap states [5–7], bistability [8], and novel lineshape behavior [9].

The microlaser/micromaser differs from conventional lasers and masers by the controlled nature of the atom-cavity interaction. Uniformity of the coupling strength between atom and cavity [10] and interaction time t_{int} of the atom through the cavity, in addition to the long lifetime of the atom upper level state compared to the transit time, create an unusual situation in which different atoms experience nearly the same interaction with the cavity. That is, interaction is nearly independent of decay and other random effects. This is in contrast to descriptions of a conventional laser [11] in which statistical averages are performed to account for the lifetimes of the excited atoms, inhomogeneous broadening, and other effects.

It is natural to ask which properties of the microlaser/micromaser persist when the restriction of a single atom is lifted. Dynamics based on single-atom quantum Rabi oscillations are not necessarily expected to hold; in addition, correlation effects may cause deviations from single-atom theory.

A related problem is to determine the effect of releasing an assumption made in analytical treatments of the microlaser/micromaser [12] that the cavity decay time is much longer than the interaction time, i.e. $\Gamma_{\text{cav}} t_{\text{int}} \ll 1$, where Γ_{cav} is the cavity linewidth and t_{int} is the interaction time. In this paper we will call this the condition of *weak decay*.

The present study was motivated by the realization that with the current experimental parameters, more than one atom at a time must be present for laser oscillation to occur. In going from the standing wave to the tilted atomic beam, uniform-coupling, traveling-wave interaction [10] the coupling strength g is decreased by a factor of 2 relative to the peak standing-wave value. The threshold number

* Tel.: +1 617 721 8180; fax: +1 617 253 4513.
E-mail address: minwah@mit.edu.

0030-4018/$ - see front matter © 2006 Elsevier B.V. All rights reserved.
doi:10.1016/j.optcom.2005.12.071

of atoms is given by [12] $N_{th} = \Gamma_{cav}/g^2 t_{int} \sim 10$. This is to be compared with $N_{th} \sim 1$ for the original (standing wave) microlaser experiment [1] if g is taken at an antinode. Therefore the study of multiple atom effects is necessary for understanding the microlaser with traveling-wave interaction.

Effects relating to nonzero $\Gamma_{cav} t_{int}$ are also of interest in the microlaser, since with present experimental parameters $\Gamma_{cav} t_{int} \sim 0.1$.

The following conventions are used in this paper. As in micromaser theory [12] we define the expected photon number $N_{ex} = r/\Gamma_{cav}$, where r is the average atom injection rate, and the pump parameter $\theta = \sqrt{N_{ex}}\, g t_{int}$, where g is the atom-field coupling.

2. Previous approaches

Two-atom events in the micromaser and microlaser were studied in [5,13] in the context of trap states. It was shown that collective events strongly degrade trap state resonances even when 99% of atoms participate in single-atom events. A more detailed theoretical treatment of two-atom events in the microlaser/micromaser was presented by Kolobov and Haake [14] via a master equation approach assuming Poisson statistics and weak decay. For $N \ll 1$ it was found that in addition to destroying trap states resonances, two-atom events generally lead to increase in mean photon number. This work was extended by Casagrande et al. to $N \approx 1$ in [15,16] via quantum trajectory simulations; a more complex perturbation to single-atom results was found.

Treatments of multi-atom behavior for $N > 1$ have generally involved strong simplifications to the atom injection scheme. D'Ariano [17] considered a micromaser pumped by clusters of up to $N = 100$ atoms which enter and leave the cavity at the same time. It was shown that for $N < N_{ex}$ the system behavior is similar to that of the one-atom maser, and for $N > N_{ex}$ the system exhibits multiple thresholds. Elk [18] considered an injection scheme in which atom arrivals are equally spaced in time. Results for small θ and $N < N_{ex}$ showed a nearly constant average photon number but a linear increase in photon number distribution width σ with N/N_{ex}. However, it is unclear what artifacts may result from the regular injection of atoms, which in general causes a reduction of photon number variance. We note that the single atom results disagree with single-atom micromaser theory [12] in both the mean and variance of the photon number distribution.

In this paper we consider the experimentally realistic case of Poissonian atom injection, and consider the effect of relaxing the condition of weak decay (note that a finite value of $\Gamma_{cav} t_{int} \sim 0.01$ was simulated in [15,16] but the effect of increasing or varying this parameter was not considered).

3. Quantum trajectory analysis

We used a quantum trajectory algorithm [19,20] in which the many-atom interaction Hamiltonian can be written

$$H = i\hbar \sum_{q=1}^{N'} g(\mathbf{r}_q)(\sigma_{q-} a^\dagger - \sigma_{q+} a) - i\hbar \frac{\Gamma_{cav}}{2} a^\dagger a, \quad (1)$$

where N' is the number of atoms in the cavity at a given time, $g(\mathbf{r}_q)$ represents the coupling strength at the position of the qth atom (for our simulations, constant g over the interaction region is assumed), $a^\dagger$ and a are photon creation and annihilation operators and $\sigma_{q\pm}$ are atom raising and lowering operators. During the simulations, N' is adjusted as atoms enter and exit the cavity randomly. Atomic decays are neglected in our simulations.

This quantum trajectory method was previously used to analyze the threshold-like transition and the possibility of many-atom effects in the original standing-wave microlaser in [21]. Readers are referred to this paper for details of the extended quantum trajectory technique also employed in the present study.

Due to limitations of computer memory and processing time, for each simulation run it was necessary to set a maximum value N_{max} for the number of atoms that could be present in the cavity at a given time. For each simulation N_{max} was at least 3 and adjusted such that the "overflow" probability was less than 1%, ensuring that the atom statistics were very close to Poissonian.

In single-atom micromaser theory [12] it is shown that, with the assumptions of single-atom events and $\Gamma_{cav} t_{int} \ll 1$ (weak decay), the steady-state photon number distribution in the cavity is given by

$$p_n = p_0 \left[\frac{n_b}{1+n_b}\right]^n \prod_{k=1}^{n} \left[1 + \frac{N_{ex} \sin^2(\sqrt{k+1}\, g t_{int})}{n_b k}\right], \quad (2)$$

where n_b is the thermal photon number and p_0 is determined by normalization. In this paper Eq. (2) will be referred to as the result from micromaser theory, though it is also applicable to the microlaser.

In this study we set thermal photon number $n_b = 0$, since for the microlaser $n_b \sim 10^{-20}$ at 300 K. The results can also be applied to the micromaser in the low temperature limit.

We performed runs of 10,000–100,000 atom injections, for varying values of N_{ex}, θ and average number of intracavity atoms $\langle N \rangle = r t_{int}$. We scaled g and Γ_{cav} as necessary to obtain the correct values for N_{ex} and θ as $\langle N \rangle$ was varied. At the beginning of each run, at least 2000 atom injections were neglected in order to allow the system to reach steady state before data collection began.

Most of our simulations were performed with $N_{ex} = 10$. This relatively small value was chosen for several reasons. First, a smaller photon number allows larger numbers of atoms to be considered, given practical limits to computer memory and processing time. Second, effects which scale as $\langle N \rangle / N_{ex}$ are more apparent for smaller N_{ex}. Finally, we observed that simulations reached steady-state distributions much more rapidly for smaller N_{ex}.

For simplicity, and to allow comparison with analytical theory, we regard g and t_{int} to be perfectly well-defined (i.e. uniform coupling and monovelocity atoms). Our QTS program has also allowed us to simulate the effects of various types of variation and broadening in a realistic system. Results of these investigations will be reported elsewhere.

The simulation was written in C and all calculations were performed on a Linux workstation. The calculations presented here required about 2000 h of CPU time.

4. Results

4.1. Single atom limit: trap states

Fig. 1 shows the average photon number as a function of θ, for $N_{ex} = 10$ and average atom number $\langle N \rangle = 0.1$ and 1.0. The depressions at $\theta_{3,1} \approx 5.65$, $\theta_{2,1} \approx 6.95$, $\theta_{1,1} \approx 9.83$ represent trap state resonances [5] described by

$$\theta_{n,q} = q\pi\sqrt{\frac{N_{ex}}{(n+1)}} \tag{3}$$

at which each atom performs exactly q Rabi oscillations and the cavity contains n photons.

With $\langle N \rangle = 0.1$ the QTS results for average photon number $\langle n \rangle$ show significantly reduced modulation due to trap states than the result of Eq. (2) although the probability of the cavity containing 2 or more atoms at any given time is only about 2%. It is only with $N = 0.01$ (data not shown) that QTS results give good agreement with micromaser theory. These results illustrate the high sensitivity of trap state resonances to 2-atom events, as described in [5]. Note that in [18] trap states are fully intact with $N = 1$ with regular injection whereas in our simulations the trap states are completely destroyed with $\langle N \rangle = 1$, further illustrating the system's sensitivity to the choice of atom injection scheme.

The photon number distributions in the low-$\langle N \rangle$ limit were verified to be in excellent agreement with Eq. (2), further confirming that the simulation was functioning properly.

4.2. Broadening of photon number distribution

Fig. 2 shows average photon numbers as a function of θ for a range of average atom numbers $\langle N \rangle$, with $N_{ex} = 10$.

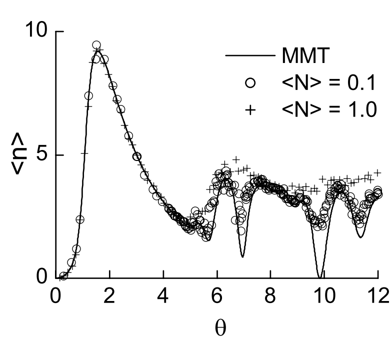

Fig. 1. Average photon number as a function of pump parameter for $\langle N \rangle = 0.1$, 1.0. For all figures, error bars are given by the scatter of data points, unless otherwise specified. Line: result from micromaser theory (Eq. (2)). $N_{ex} = 10$.

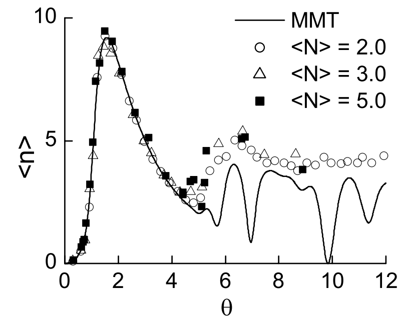

Fig. 2. Simulation results for average photon number vs. pump parameter. Solid line, result from Eq. (2).

Figs. 3 and 4 show corresponding values of Mandel parameter

$$Q \equiv \frac{(\langle n^2 \rangle - \langle n \rangle^2)}{\langle n \rangle} - 1. \tag{4}$$

For $\langle N \rangle = 0.01$, excellent agreement with Eq. (2) was found (data not shown). Note that for larger values of θ, Q is large and may be difficult to interpret due to the presence of two or more peaks in the photon number distribution.

For $\theta < 5$, before the onset of trap state resonances, the results for average photon number remain remarkably

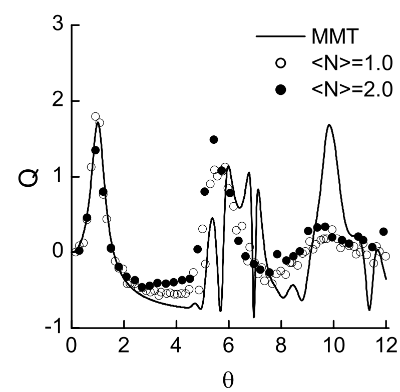

Fig. 3. Simulation results for Q parameter vs. pump parameter. Solid line, result from Eq. (2).

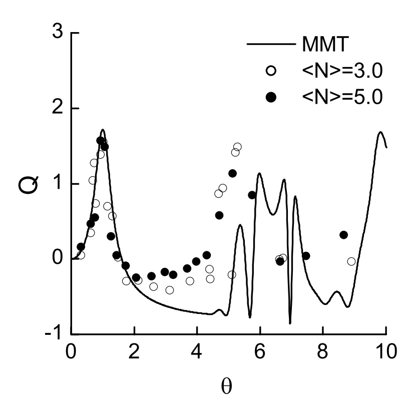

Fig. 4. Simulation results for Q parameter vs. pump parameter. Solid line, result from Eq. (2).

close to the prediction of micromaser theory. The values for Q, however, show a increase with $\langle N \rangle$ in the range $2 < \theta < 5$. This interval corresponds to the region in micromaser theory predicts sub-Poisson statistics ($Q < 0$).

Similar increases in Q are observed in a small interval near $\theta = 8$, between two trap states. Simulations with $N_{ex} = 30$ and 50, in which trap state resonances are more narrow, showed similar behavior over wider intervals between trap states.

The parameter Q was calculated as a function of $\langle N \rangle / N_{ex}$, with $\theta = 3$, for $N_{ex} = 5$, 10, 15, 30. The increase of Q is seen to be linear with $\langle N \rangle / N_{ex}$; for $N_{ex} \geqslant 5$ we find (Fig.5) that the dependence of Q on $\langle N \rangle / N_{ex}$ may be approximately described by

$$Q \approx Q_0(N_{ex}, \theta) + \alpha(\theta)(\langle N \rangle / N_{ex}), \tag{5}$$

where Q_0 is the value of the Mandel parameter from micromaser theory.

We find $\alpha(\theta = 3) \approx 0.80 \pm .05$. By comparison, a linear fit to the data from Elk's study using regular atom injection [18] with $N > 1$ for $N_{ex} = 10{,}30$, $n_b = 0.1$, and $\theta = 3$ gives a comparable but smaller value of $\alpha(\theta = 3) \approx 0.63 \pm .02$. It is perhaps not surprising that regular atom injection leads to a reduced photon number variance compared to Poisson injection. In addition, it appears that the excess variance proportional to $\langle N \rangle / N_{ex}$ is also reduced for a regular injection scheme.

Fig. 6 shows $\alpha(\theta)$ calculated via a least-squares linear fit with $N_{ex} = 10$ and $\langle N \rangle = 0$, 0.2, 0.4, 0.6, 0.8, 2. Error bars indicate the degree of linearity between Q and $\langle N \rangle / N_{ex}$ (see caption). Note that α and Q tend to have opposite signs. Values of α are generally positive for θ where the single-atom, weak-decay theory predicts sub-Poisson statistics. For many values of θ (for example $4.8 < \theta < 5.8$) the dependence of Q with $\langle N \rangle / N_{ex}$ is nonlinear and even nonmonotonic; in these cases Eq. (5) does not hold. Nevertheless, we present the results of the linear fit in Fig. 6 simply to give an indication of the positive or negative trend of the dependence of Q on $\langle N \rangle / N_{ex}$.

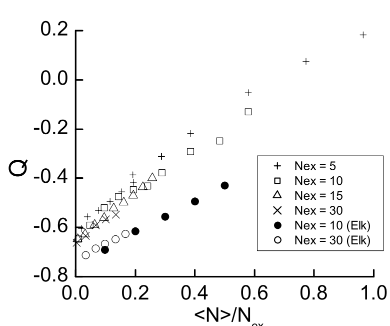

Fig. 5. Simulation results for Q parameter vs. $\langle N \rangle / N_{ex}$, for varying N_{ex} and $\theta = 3$. Filled and open circles: results from regular injection model of Elk with $N_{ex} = 10{,}30$, $n_b = 0.1$, and $\theta = 3$ [18].

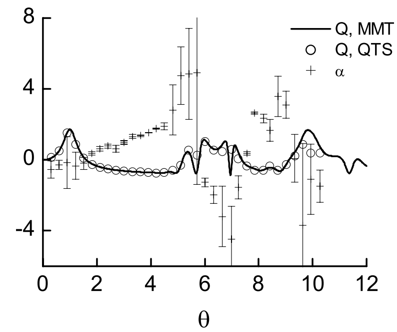

Fig. 6. Solid line: Q parameter from Eq. (2); Circles: fitting parameter Q_0 from simulation data and Eq. (5), as described in text; Crosses: fitting parameter α from Eq. (5). Error bars indicate the degree of linearity of Q with $\langle N \rangle / N_{ex}$; error bar length is twice the standard error of the slope of a linear fit.

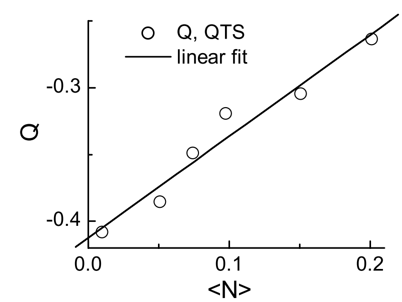

Fig. 7. Points: simulation results for increase in Q with $N_{ex} = 1$. Line: linear fit $Q = -0.412(\pm .009) + 0.759(\pm .082) \langle N \rangle$.

4.3. Many-atom vs. finite transit time effects

In [18] the increase of variance proportional to $\langle N \rangle / N_{ex}$ was interpreted as being due to many-atom interactions. We note, however, that $\langle N \rangle / N_{ex}$ is equal to simply $t_{int}\Gamma_{cav}$, a parameter describing cavity decay during the transit time, and is not directly related to the number of atoms. The extra variance observed in this study and by Elk can therefore be seen as a consequence not of multiple atoms, but of cavity decay during an atom's transit time. For example, we may have $\langle N \rangle \gg 1$ but virtually no extra variance if $N_{ex} \gg \langle N \rangle$. More importantly, there are examples in which $\langle N \rangle \ll 1$ but excess variance still occurs. Fig. 7 shows Q as a function of $\langle N \rangle$ for $N_{ex} = 1$, $\theta = 2$. A linear increase in variance is seen even for $\langle N \rangle < 0.1$.

5. Conclusions

Our calculations have clarified the distinction between many-atom effects and effects due to cavity decay during transit-time. Many-atom events destroy the trap state resonances and therefore have strong effects for parameters for which these resonances are prominent. This effect had been shown earlier by a number of analytical and numerical studies [14–16]. Away from these resonances, the system shows remarkable agreement with single-atom micromaser theory. However, for values of θ for which micromaser theory predicts sub-Poisson statistics, cavity decay during transit time cause an increase in variance relative to micromaser theory, by an amount approximately proportional to $\langle N\rangle/\ N_{\rm ex} = t_{\rm int}\Gamma_{\rm cav}$.

Comparing our results with those of the regular injection model of Elk [18], we find the Poisson-injection system displays both an increased photon number variance and an increase in the slope of the excess variance. In the study of D'Ariano of a micromaser pumped by atom clusters [17], no discernible increase in photon number variance is seen for a atom cluster size less than $N_{\rm ex}$.

Lack of collective effects away from trap states may be a consequence of the noncorrelated Rabi phases of atoms which have entered the cavity at different times. Increase of variance may represent a decrease in magnitude of negative differential gain in the atom-cavity system. Future work will include development of models to give insight into the mechanisms of these effects.

Acknowledgements

The author thanks Michael S. Feld, Kyungwon An, and Chung-Chieh Yu for many helpful discussions. This work was supported by National Science Foundation grants 9876974-PHY and 0111370-CHE.

References

[1] K. An, J.J. Childs, R.R. Dasari, M.S. Feld, Phys. Rev. Lett. 73 (1994) 3375.
[2] C. Fang-Yen, Multiple Thresholds and Many-Atom Dynamics in the Cavity QED Microlaser. Ph. D. thesis, Massachusetts Institute of Technology, 2002.
[3] D. Meschede, H. Walther, G. Muller, Phys. Rev. Lett. 54 (1985) 551.
[4] G. Rempe, F. Schmidt-Kaler, H. Walther, Phys. Rev. Lett. 64 (1990) 2783.
[5] P. Meystre, G. Rempe, H. Walther, Opt. Lett. 13 (1988) 1078.
[6] M. Weidinger, B.T.H. Varcoe, R. Heerlein, H. Walther, Phys. Rev. Lett. 82 (1999) 3795.
[7] S. Brattke, B.T.H. Varcoe, H. Walther, Phys. Rev. Lett. 86 (2001) 3534.
[8] O. Benson, G. Raithel, H. Walther, Phys. Rev. Lett. 72 (1994) 3506.
[9] M.O. Scully, H. Walther, G.S. Agarwal, T. Quang, W. Schleich, Phys. Rev. A 44 (1991) 5992.
[10] K. An, R.R. Dasari, M.S. Feld, Opt. Lett. 22 (1997) 1500.
[11] M. Sargent, M. Scully, W. Lamb, Quantum Optics, Addison-Wesley, 1974.
[12] P. Filipowicz, J. Javanainen, P. Meystre, Phys. Rev. A 34 (1986) 3077.
[13] E. Wehner, R. Seno, N. Sterpi, B.-G. Englert, H. Walther, Opt. Commun. 110 (1994) 655.
[14] M.I. Kolobov, F. Haake, Phys. Rev. A 55 (1997) 3033.
[15] F. Casagrande, A. Lulli, S. Ulzega, Phys. Lett. A 255 (1999) 133.
[16] F. Casagrande, A. Lulli, S. Ulzega, Phys. Rev. A 60 (1999) 1582.
[17] G.M. D'Ariano, N. Sterpi, A. Zucchetti, Phys. Rev. Lett. 74 (1995) 900.
[18] M. Elk, Phys. Rev. A 54 (1996) 4351.
[19] J. Dalibard, Y. Castin, K. Mølmer, Phys. Rev. Lett. 68 (1991) 580.
[20] H.J. Carmichael, Phys. Rev. Lett. 70 (1993) 2273.
[21] C. Yang, K. An, Phys. Rev. A 55 (1997) 4492.